

Self-Assembly of Organic–Inorganic Hybrid Materials Constructed from Eight-Connected Coordination Polymer Hosts with Nanotube Channels and Polyoxometalate Guests As Templates

Xiuli Wang,* Yanfeng Bi, Baokuan Chen, Hongyan Lin, and Guocheng Liu

Faculty of Chemistry and Chemical Engineering, Bohai University, Jinzhou 121000, P.R. China

Received July 22, 2007

Two polyoxometalate-templated organic–inorganic hybrid porous frameworks, namely, $[\text{Cu}_2(\text{H}_2\text{O})_2(\text{bpp})_2\text{Cl}][\text{PM}_{12}\text{O}_{40}] \cdot \sim 20\text{H}_2\text{O}$ (for **1**, $M = \text{W}$; for **2**, $M = \text{Mo}$; $\text{bpp} = 1,3\text{-bis}(4\text{-pyridyl})\text{propane}$), were self-assembly obtained and structurally determined by elemental analyses, inductively coupled plasma analyses, infrared spectroscopy, and single-crystal X-ray diffraction analyses. Single-crystal X-ray analysis of these crystals revealed that both of the structures are constructed from eight-connected three-dimensional coordination polymer hosts $[\text{Cu}_2(\text{H}_2\text{O})_2(\text{bpp})_2\text{Cl}]_n^{3n+}$ and ball-shaped Keggin-type guests $[\text{PM}_{12}\text{O}_{40}]_n^{3n-}$ as templates. The polymer hosts resulted from a bcc-type framework with nanotubes, and the nanotubes can be regarded as a tetra-stranded helix structure. Furthermore, compounds **1** and **2** exhibit photoluminescent properties at ambient temperature, and the compound **2** bulk-modified carbon paste electrode (**2**-CPE) displays good electrocatalytic activity toward the reduction of nitrite.

Introduction

The significant contemporary interest in metal-organic frameworks (MOFs) reflects a structural and compositional diversity that endows these materials with a range of physical properties that yield applications to catalysis, molecular adsorption, optical, and electronic and magnetic materials.¹ Among the large amount of reported work, the rational synthesis of MOFs containing nanoscale caves is of particular interest, and the numbers of host frameworks of such materials which can facilitate the removal/adsorption of guest molecules has rapidly grown.^{2,3} However, despite the practical and fundamental importance of these materials, the designed synthesis of such materials remains an elusive goal.^{2c,4} Anions are capable of directing the formation of some porous entities through either cation–anion interactions

or hydrogen-bonding interactions between an organic host and an anionic guest; thus, a current important synthetic strategy in this field is the use of large inorganic anions as templates to build novel organic–inorganic hybrid frameworks.⁵ In this aspect, polyoxometalates (POMs), because of their controllable shape, size, and high negative charges, as well as their diverse electronic, magnetic, photochemical, and catalytic properties, have been regarded as suitable anionic templates to build cationic coordination polymer

* To whom correspondence should be addressed. Email: wangxiuli@bhu.edu.cn. Tel: +86-416-3400158. Fax: +86-416-3400158.

- (1) (a) Hagrman, P. J.; Hagrman, D.; Zubieta, J. *Angew. Chem. Int. Ed.* **1999**, *38*, 2638–2684. (b) Swiegers, G. F.; Malefete, T. J. *Chem. Rev.* **2000**, *100*, 3483–3538. (c) Kitaura, S.; Kitagawa, R.; Kubota, Y.; Kobayashi, T. C.; Kindo, K.; Mita, Y.; Matsuo, S.; Kobayashi, M.; Chang, H. C.; Ozawa, T. C.; Suzuki, M.; Sakata, M.; Takata, M. *Science* **2002**, *298*, 2358–2361. (d) Cheetham, A. J. *Science* **1994**, *264*, 794–795.
- (2) (a) Turro, N. *Acc. Chem. Res.* **2000**, *33*, 637–646. (b) Eddaoudi, M.; Moler, D. B.; Li, H. L.; Chen, B. L.; Reineke, T. M.; O’Keeffe, M.; Yaghi, O. M. *Acc. Chem. Res.* **2001**, *34*, 319–330. (c) Pan, L.; Liu, H. M.; Lei, X. G.; Huang, X. Y.; Olson, D. H.; Turro, N. J.; Li, J. *Angew. Chem. Int. Ed.* **2003**, *42*, 542–543.

- (3) (a) Corma, A.; Forns, V.; Garcia, H.; Miranda, M. A.; Sabater, M. J. *J. Am. Chem. Soc.* **1994**, *116*, 9767–9768. (b) Eddaoudi, M.; Kim, J.; Rosi, N.; Vodak, D.; Wachter, J.; Keffe, M. O.; Yaghi, O. M. *Science* **2002**, *295*, 469–472. (c) Seo, J.; Whang, S. D.; Lee, H.; Jun, S. I.; Oh, J.; Jeon, Y.; Kim, J.; Eddaoudi, K. *Nature* **2000**, *404*, 982. (d) Rosi, N.; Eckert, L. J.; Vodak, M. D.; Kim, T. J.; O’Keeffe, M.; Yaghi, O. M. *Science* **2003**, *300*, 1127–1129.
- (4) (a) Liu, S. X.; Hua, X. L.; Gao, B.; Zhang, C. D.; Sun, C. Y.; Li, D. H.; Su, Z. M. *Chem. Commun.* **2005**, 5023, 5025. (b) Kesanli, B.; Cui, Y.; Smith, M. R.; Bittner, E. W.; Bockrath, B. C.; Lin, W. B. *Angew. Chem. Int. Ed.* **2005**, *44*, 72–75. (c) Cui, Y.; Lee, S. J.; Lin, W. B. *J. Am. Chem. Soc.* **2003**, *125*, 6014–6015. (d) Kitagawa, S.; Kitaura, R.; Noro, S. *Angew. Chem. Int. Ed.* **2004**, *43*, 2334–2375.
- (5) (a) Hagrman, P. J.; Hagrman, D.; Zubieta, J. *Angew. Chem. Int. Ed.* **1999**, *38*, 2638–2684; and references therein. (b) Holman, K. T.; Halihan, M. M.; Jurisson, S. S.; Atwood, J. L.; Burkhalter, R. S.; Mitchell, A. R.; Steed, J. W. *J. Am. Chem. Soc.* **1996**, *118*, 9567–9576. (c) Hagrman, D.; Hagrman, P.; Zubieta, J. *Angew. Chem. Int. Ed.* **1999**, *38*, 3165–3168. (d) Vilar, R.; Mingos, D. M. P.; White, A. J. P.; Williams, D. J. *Angew. Chem. Int. Ed.* **1998**, *37*, 1258–1261. (e) Bianchi, G.; Garcia-España, E.; Bowman-James, K. *Supramolecular Chemistry of Anions*; Wiley-VCH: Weinheim, 1997.

hosts or organic–inorganic hybrid materials.^{6–8} However, up to now, it is surprising that relatively little progress has been made in this interesting field to prepare high-connected and high-dimensional POM-templated porous open-MOFs, although POM chemistry has touched an almost unprecedented number of other fields of chemistry.⁹ Recently, several extended structures of cationic coordination networks suggest that the introduction of neutral N-donor organic ligands usually leads to the formation of cationic metal-organic complex segments which might satisfy the requirements for POM-templated assembly.^{7c–h,8,10} Hence, the use of long flexible bridging ligand 1,3-bis(4-pyridyl)propane (bpp), which maybe facilitate the formation of large voids, was fully considered in our synthetic efforts for new POM-templated organic–inorganic hybrid porous compounds. Herein, we report the synthesis, structures, and properties of two unprecedented organic–inorganic hybrid porous frameworks, namely, $[\text{Cu}_2(\text{H}_2\text{O})_2(\text{bpp})_2\text{Cl}][\text{PM}_{12}\text{O}_{40}] \cdot \sim 20\text{H}_2\text{O}$ (for **1**, M = W; for **2**, M = Mo). Single-crystal X-ray analysis of these crystals revealed that both of the structures are constructed from eight-connected coordination polymer hosts $[\text{Cu}_2(\text{H}_2\text{O})_2(\text{bpp})_2\text{Cl}]_n^{3n+}$ and ball-shaped Keggin-type guests $[\text{PM}_{12}\text{O}_{40}]_n^{3n-}$ as templates.

Experimental Section

Materials and Measurements. All reagents were purchased from commercial sources and used as received. Fourier transform infrared (FT-IR) spectra (KBr pellets) were taken on a Magna FT-IR 560 spectrometer. Elemental analyses (C, H, and N) were performed on a Perkin-Elmer 2400 CHN elemental analyzer. P, W, Mo, and Cu were determined by a Leaman inductively coupled plasma (ICP) spectrometer. Powder X-ray diffraction (XRD) was

Table 1. Crystal Data and Structure Refinement for Complexes **1** and **2**

	1	2
formula	$\text{C}_{52}\text{H}_{100}\text{ClCu}_2\text{N}_8\text{O}_{62}\text{PW}_{12}$	$\text{C}_{52}\text{H}_{95.50}\text{ClCu}_2\text{N}_8\text{O}_{62}\text{PMo}_{12}$
formula wt	4229.10	3169.64
cryst syst	tetragonal	tetragonal
space group	$P4(2)/n$	$P4(2)/n$
<i>a</i> (Å)	24.1547(8)	24.2146(12)
<i>b</i> (Å)	24.1547(8)	24.2146(12)
<i>c</i> (Å)	18.6783(8)	18.6339(12)
<i>V</i> (Å ³)	10897.8(7)	10925.9(10)
<i>Z</i>	4	4
<i>D_c</i> (g cm ⁻³)	2.578	1.927
<i>μ</i> (mm ⁻¹)	13.121	1.841
<i>F</i> (000)	7768.0	6214.0
tot. data	54349	53253
uniq. data	9588	9475
<i>R</i> _{int}	0.109	0.065
GOF	1.108	1.099
<i>R</i> ₁ ^a [<i>I</i> > 2σ(<i>I</i>)]	0.0584	0.0720
<i>wR</i> ₂ ^b (all data)	0.1749	0.2161

$$^a R_1 = \sum \Delta F_o / \sum |F_o|, \quad ^b wR_2 = [\sum (w(F_o^2 - F_c^2)^2) / \sum w(F_o^2)^2]^{1/2}.$$

determined by a Bruker D8 Advance diffractometer. Fluorescence spectra were performed on a Hitachi F-4500 fluorescence/phosphorescence spectrophotometer with a 450 W xenon lamp as the excitation source. Thermogravimetric (TG) analyses were performed on a Pyris-Diamond TG/DAT instrument in flowing N₂ with a heating rate of 10 °C /min. A CHI 440 electrochemical workstation connected to a Digital-586 personal computer was used for control of the electrochemical measurements and for data collection.

Synthesis of Complexes 1 and 2. A mixture of $\text{CuCl}_2 \cdot 2\text{H}_2\text{O}$ (18 mg, 0.1 mmol) in ethanol (5 mL) and bpp (10 mg, 0.05 mmol) in acetic acid (5 mL) was stirred in air for 0.5 h; then a dimethylformamide (DMF) solution (6 mL) of $\text{H}_3\text{PW}_{12}\text{O}_{40} \cdot \sim 24\text{H}_2\text{O}$ (ca. 65 mg, 0.02 mmol) was slowly diffused into the mixture over 2 h at 70 °C. The resulting solutions were filtered, and the filtrates were allowed to stand in air at room temperature for several days, yielding the dark-blue crystals of **1** (yield: ca. 30% based on W). Elemental analysis (%) calcd. for $\text{C}_{52}\text{H}_{100}\text{ClCu}_2\text{N}_8\text{O}_{62}\text{PW}_{12}$: C, 14.77; H, 2.36; N, 2.65; P, 0.73; W, 52.15; Cu, 3.23%. Found: C, 14.80; H, 2.37; N, 2.61; P, 0.69; W, 52.20; Cu, 3.25%. The synthesis method of **2** is similar to that for **1** except for $\text{H}_3\text{PMo}_{12}\text{O}_{40} \cdot \sim 20\text{H}_2\text{O}$ (ca.45 mg, 0.02 mmol) as the substitute of $\text{H}_3\text{PW}_{12}\text{O}_{40} \cdot \sim 24\text{H}_2\text{O}$. Yield: about 43% based on Mo. Elemental analysis (%) calcd. for $\text{C}_{52}\text{H}_{95.50}\text{ClCu}_2\text{N}_8\text{O}_{62}\text{PMo}_{12}$: C, 19.69; H, 3.01; N, 3.53; P, 0.98; Mo, 36.32; Cu, 4.01%. Found: C, 19.80; H, 3.10; N, 3.51; P, 0.94; Mo, 36.25; Cu, 4.05%.

X-ray Crystallographic Analysis. All diffraction data were collected using a Bruker APEX diffractometer (Mo Kα radiation, graphite monochromator, $\lambda = 0.71073$ Å). Data were corrected for Lorentz and polarization effects, and equivalent data were averaged. The structures were solved by direct methods and refined by the full-matrix least-squares method on *F*² with the SHELXL-97 software.¹¹ All nonhydrogen atoms except some disordered water molecules were refined anisotropically, and the hydrogen atoms of the ligands were generated theoretically onto the specific atoms and refined isotropically with fixed thermal factors. All the crystal data and structure refinement details for the two compounds are given in Table 1. The Supporting Information Table S1 lists the data of selected bond distances and angles. Crystallographic data for the structures reported in this paper have been deposited in the

- (6) (a) Hill, C. L. *Chem. Rev.* **1998**, *98*, 1–2. (b) *Polyoxometalate Chemistry: From Topology Via Self-Assembly to Applications*; Pope, M. T., Müller, A., Eds.; Kluwer: Dordrecht, The Netherlands, 2001. (c) *Polyoxometalate Chemistry for Nano-Composite Design*; Yamase, T., Pope, M. T., Eds.; Kluwer: Dordrecht, The Netherlands, 2002.
- (7) (a) Hagrman, D.; Zubieta, J. *Chem. Commun.* **1998**, *2005*, 2006. (b) Zheng, L. M.; Wang, Y. S.; Wang, X. Q.; Korp, J. D.; Jacobson, A. J. *Inorg. Chem.* **2001**, *40*, 1380–1385. (c) Inman, C.; Knaust, J. M.; Keller, S. W. *Chem. Commun.* **2002**, *156*, 157. (d) Knaust, J. M.; Inman, C.; Keller, S. W. *Chem. Commun.* **2004**, *492*, 493. (e) Ren, Y. P.; Kong, X. J.; Hu, X. Y.; Sun, M.; Long, L. S.; Huang, R. B.; Zheng, L. S. *Inorg. Chem.* **2006**, *45*, 4016–4023. (f) Lisnard, L.; Dolbecq, A.; Mialane, P.; Marrot, J.; Codjovi, E.; Sécheresse, F. *Dalton Trans.* **2005**, *3913*, 3920. (g) Kong, X. J.; Ren, Y. P.; Zheng, P. Q.; Long, Y. X.; Long, L. S.; Huang, R. B.; Zheng, L. S. *Inorg. Chem.* **2006**, *45*, 10702–10711. (h) Jin, H.; Qi, Y. F.; Wang, E. B.; Li, Y. G.; Wang, X. L.; Qin, C.; Chang, S. *Eur. J. Inorg. Chem.* **2006**, *4541*, 4545. (i) Wei, M.; He, C.; Hua, W.; Duan, C.; Li, S.; Meng, Q. *J. Am. Chem. Soc.* **2006**, *128*, 13318–13319.
- (8) (a) Sun, C. Y.; Li, Y. G.; Wang, E. B.; Xiao, D. R.; An, H. Y.; Xu, L. *Inorg. Chem.* **2007**, *46*, 1563–1574. (b) Uehara, K.; Kasai, K.; Mizuno, N. *Inorg. Chem.* **2007**, *46*, 2563–2570. (c) Li, Y. G.; Dai, L. M.; Wang, Y. H.; Wang, X. L.; Wang, E. B.; Su, Z. M.; Xu, L. *Chem. Commun.* **2007**, *259*, 3–2595. (d) Wei, M. L.; He, C.; Sun, Q. Z.; Meng, Q. J.; Duan, C. Y. *Inorg. Chem.* **2007**, *46*, 5957–5966.
- (9) (a) Pgerler, P. K.; Cronin, L. *Angew. Chem. Int. Ed.* **2005**, *44*, 844–846. (b) Wang, X. L.; Qin, C.; Wang, E. B.; Su, Z. M.; Li, Y. G.; Xu, L. *Angew. Chem. Int. Ed.* **2006**, *45*, 7411–7414.
- (10) (a) Feng, S. H.; Xu, R. R. *Acc. Chem. Res.* **2001**, *34*, 239–247; and references therein. (b) Zheng, L. M.; Whitfield, T.; Wang, X.; Jacobson, A. J. *Angew. Chem. Int. Ed.* **2000**, *39*, 4528–4531. (c) Lü, J.; Shen, E. H.; Yuan, M.; Li, Y. G.; Wang, E. B.; Hu, C. W.; Xu, L.; Peng, J. *Inorg. Chem.* **2003**, *42*, 6956–6958. (d) Li, Y. G.; De, G.; Yuan, M.; Wang, E. B.; Huang, R. D.; Hu, C. W.; Hu, N. H.; Jia, H. Q. *Dalton Trans.* **2003**, *331*, 334.

- (11) (a) Sheldrick, G. M. *SHELXS-97, Program for Crystal Structure Solution*; University of Göttingen: Germany, 1997. (b) Sheldrick, G. M. *SHELXL-97, Program for Crystal Structure Refinement*; University of Göttingen: Germany, 1997.

Cambridge Crystallographic Data Center with CCDC reference numbers 647981 and 649312 for compounds **1** and **2**, respectively.

Results and Discussion

Preparation of Complexes. The self-assembly reaction of CuCl_2 with 1,3-bis(4-pyridyl)propane and $\text{H}_3\text{PM}_{12}\text{O}_{40}$ in the DMF–HOAc–EtOH mixed solution is an effective route for the preparation of novel POM-templated organic–inorganic hybrid materials. The isolation of the title compounds mainly depends on solvent system and temperature. If the reaction was performed in HOAc–EtOH mixed solvent system, we could not obtain the expected single-crystal but only a precipitate. If HOAc was not added into the reaction system, a lot of green precipitate was obtained. So DMF and HOAc may be prerequisite for the formation of the title compounds as a single crystalline solid. If the reaction is performed at room temperature or at lower than $70\text{ }^\circ\text{C}$, only a precipitate can be obtained.

Most reported POM-based materials, especially obtained under hydrothermal conditions, show that POMs tend to coordinate to metal centers.^{9b} We obtained two novel three-dimensional (3-D) coordination polymer hosts encapsulating noncoordinating $[\text{PM}_{12}\text{O}_{40}]^{3-}$ guests, which can be attributed to the template effect of the POM, and is similar to previous reports.⁸

Description of Crystal Structures. The building units of both compounds consist of two Cu^{II} centers, a noncoordinating $[\text{PM}_{12}\text{O}_{40}]^{3-}$ cluster, a coordinated chloride ion, four bpp ligands, two coordinated water molecules, and other disordered water molecules (Figure 1 and Supporting Information Figure S1). An analysis of the local symmetry of the equivalent Cu^{II} center reveals that the Cu1 center is bound to four bpp nitrogen atoms, a coordinated chlorine atom, and one coordinated water molecule adopting a distorted octahedral CuClN_4O coordination geometry. Each Cu1 atom is weakly coordinated by a water molecule and a chlorine atom (for **1**, $\text{Cu}(1)\text{--O}(1\text{W}) = 2.826(3)\text{ \AA}$, $\text{Cu}(1)\text{--Cl}(1) = 2.716(3)\text{ \AA}$; for **2**, $\text{Cu}(1)\text{--O}(1\text{W}) = 2.813(2)\text{ \AA}$, $\text{Cu}(1)\text{--Cl}(1) = 2.722(2)\text{ \AA}$) resulting from a strong Jahn–Teller effect.¹² Except for the coordinated water molecules and chlorine atom, all nitrogen atoms form reasonably strong bonds with the copper atoms in the range between $1.979(17)$ and $2.035(17)\text{ \AA}$. The $[\text{PM}_{12}\text{O}_{40}]^{3-}$ anions possess the well-known Keggin-type structures, and all the bond lengths and angles are within the normal ranges and in close agreement with those described in the literature (Supporting Information Table S1).^{7c–e,8c,9b}

From further analysis of the structures of the title compounds, five unique features are apparent: (1) an eight-connected Cu_2 -cluster building unit; (2) a 3-D cationic network with a body-centered cubic (bcc) topology; (3) nanotube channels with tetra-stranded helix; (4) nanoscale open windows and large channel system with an extra-framework volume of about 36%; (5) potential functionalization sites both on the copper atoms and on the $[\text{PM}_{12}\text{O}_{40}]^{3-}$ clusters.

Two octahedral Cu^{II} cores share one chlorine atom to form a dinuclear building unit. Interestingly, each dinuclear unit

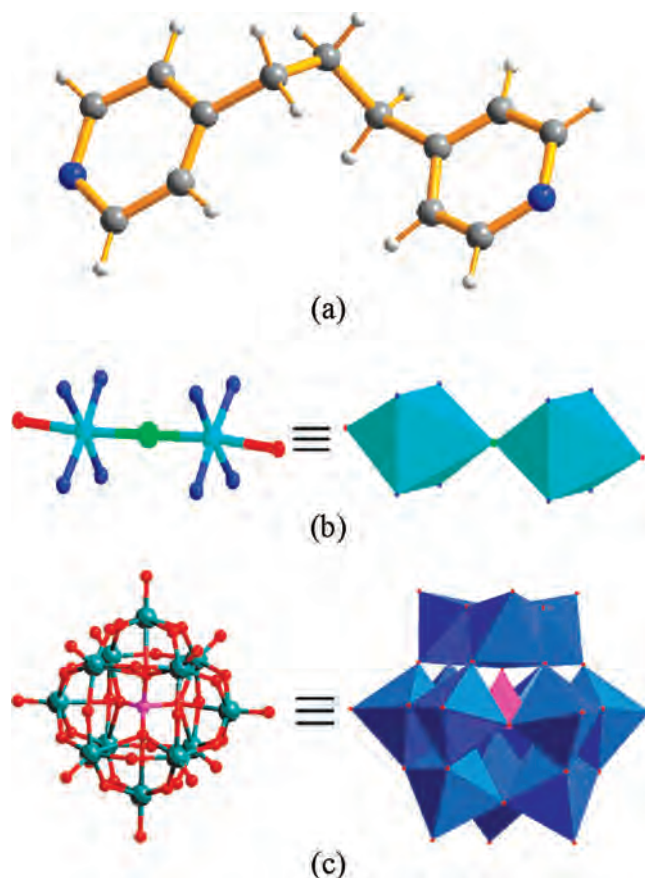


Figure 1. Building units in **1** and **2**. (a) Ball-and-stick representation of the long flexible bridging ligand bpp. N, blue; C, gray; H, white. (b) Ball-and-stick (left) and polyhedral (right) representations of the building block of the dinuclear unit. Cu, cyan; Cl, green; N, blue. (c) Ball-and-stick (left) and polyhedral (right) representations of Keggin-type cluster $[\text{PM}_{12}\text{O}_{40}]^{3-}$. M, darkgreen; P and polyhedron PO_4 , purple; polyhedra MO_6 , blue.

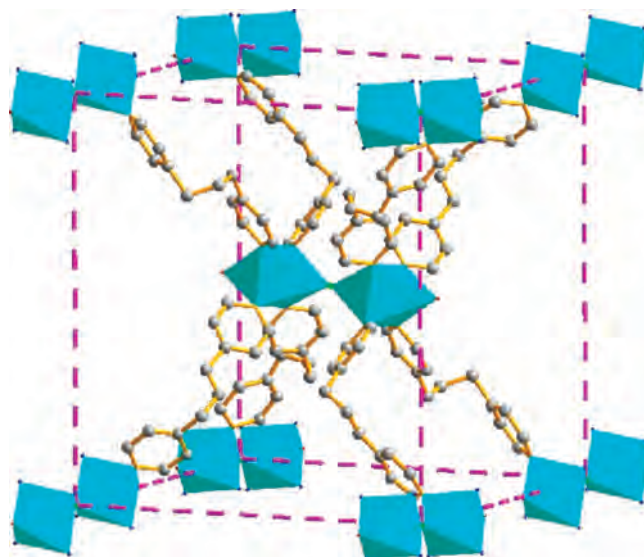


Figure 2. View of the linkages of a dinuclear unit with eight adjacent neighbors showing a body-centered cube.

is further linked to eight nearest-neighbors, with distances of 15.3 \AA , through eight bpp ligands, thus resulting in a 3-D bcc-type cationic framework (Figure 2). The connectivity is remarkably similar to the first eight-connected CsCl-type example found in the coordination network in which the

single La^{III} is well surrounded by eight 4,4'-bipyridine- $\text{N,N}'$ -dioxide ligands.¹³ It is worth noting that the unique dinuclear Cu_2 -cluster building unit, to the best of our knowledge, has not been reported so far, although other mono-, tri-, and multinuclear eight-connected clusters have been reported in coordination chemistry.^{12–14}

Further insight into the nature of this intricate architecture of a nanotube channel with dimension of $6.1 \text{ \AA} \times 11.7 \text{ \AA}$ (code A, measured between opposite atoms, hereafter) will be found. Interestingly, the nanotube channel also can be regarded as a tetra-stranded helix structure which has never been observed so far in coordination chemistry (Supporting Information Figure S2).¹⁵ To be pointed out, such a novel structure, served with weak coordinated water molecules and guest water molecules, is a potential candidate for a microreactor with metal-containing active sites. These sites in crystalline porous materials have functionalities that could permit molecular recognition, catalysis, or gas storage.^{12,16} The nanotube channel was further linked toward four directions by chlorine atoms to form another kind of channel with dimension of $8.1 \text{ \AA} \times 17.1 \text{ \AA}$ (code B) along the [001] direction (Figure 3). Additionally, two other kinds of large channels also can be observed along the [110] direction with dimension of $13.8 \text{ \AA} \times 14.6 \text{ \AA}$ (code C) and $13.9 \text{ \AA} \times 12.5 \text{ \AA}$ (code D), respectively (Figure 4). Strictly speaking, only channels C and D are large enough to accommodate the Keggin-type ion (ca. $10.4 \times 10.4 \text{ \AA}$) into an octahedral pocket while channels A and B are not (Supporting Information Figure S3). It is supposed that Keggin-type ions may serve as templates during the assembly so that hybrid cationic building blocks are aggregated around them, leading to the large porous 3-D cationic framework. The cationic structures of the title compounds reflect not only the flexible geometry of the bpp building block and the POM-templates but also the coordination preferences of the Cu^{II} sites that adopt the conventional $4 + 2$ coordination geometries enhanced by

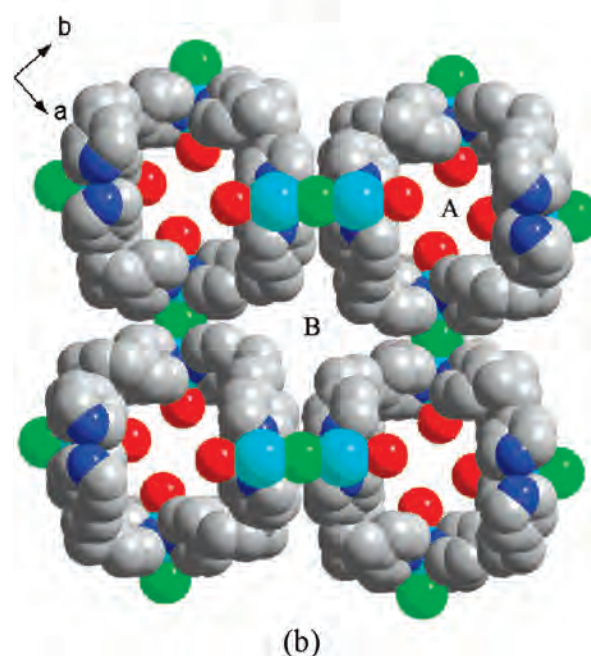
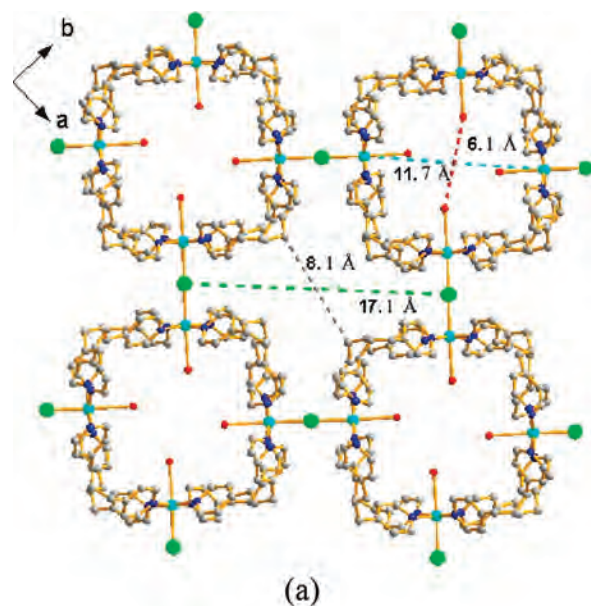


Figure 3. Ball-and-stick (a) and space-filling (b) representations of the channels in the 3-D cationic structure along the [001] direction. The channel sizes are dependent on the distance between Cu, Cl, O1W on the Cu centers, and C24 derived from bpp ligands and their symmetric operation atoms, respectively. The H atoms, the solvent–water molecules, and the Keggin-type ion templates are omitted for clarity.

the presence of the weak coordinated water molecules and chlorine atoms.

Another important structural feature results from the noncoordinating $[\text{PM}_{12}\text{O}_{40}]^{3-}$ templates which are arranged in a face-centered cubic (fcc-type) supramolecular structure via $\text{C}-\text{H}\cdots\text{O}$ interactions between bpp ligands and oxygen atoms from adjacent POMs in the range of $3.16\text{--}3.46 \text{ \AA}$ (Figure 5).¹⁷ More importantly, the large open channels (with dimensions of $6.1 \text{ \AA} \times 6.1 \text{ \AA}$ and $8.1 \text{ \AA} \times 8.1 \text{ \AA}$, based on channel A and B, respectively) generated within these copper–bpp tubes and $[\text{PM}_{12}\text{O}_{40}]^{3-}$ clusters are populated by diffuse, disordered water molecules, as established by

- (12) Luo, T. T.; Tsai, H. L.; Yang, S. L.; Liu, Y. H.; Yadav, D. R.; Su, C. C.; Ueng, C. H.; Lin, L. G.; Lu, K. L. *Angew. Chem. Int. Ed.* **2005**, *44*, 6063–6067.
- (13) Long, D. L.; Blake, A. J.; Champness, N. R.; Wilson, C.; Schröder, M. *Angew. Chem. Int. Ed.* **2001**, *40*, 2443–2447.
- (14) (a) Chun, H.; Kim, D.; Dybtsev, D. N.; Kim, K. *Angew. Chem. Int. Ed.* **2004**, *43*, 971–974. (b) Hill, R. J.; Long, D. L.; Hubberstey, P.; Schröder, M.; Champness, N. R. *J. Solid State Chem.* **2005**, *178*, 2414–2419. (c) Long, D. L.; Hill, R. J.; Blake, A. J.; Champness, N. R.; Hubberstey, P.; Proserpio, D. M.; Wilson, C.; Schröder, M. *Angew. Chem. Int. Ed.* **2004**, *43*, 1851–1854. (d) Fang, Q. R.; Zhu, G. S.; Jin, Z.; Xue, M.; Wei, X.; Wang, D. J.; Qiu, S. L. *Angew. Chem. Int. Ed.* **2006**, *45*, 6126–6130. (e) Pan, L.; Liu, H. M.; Lei, X. G.; Huang, X. Y.; Olson, D. H.; Turro, N. J.; Li, J. *Angew. Chem. Int. Ed.* **2003**, *42*, 542–546. (f) Wang, X. L.; Qin, C.; Wang, E. B.; Su, Z. M. *Chem.–Eur. J.* **2006**, *12*, 5823–5831. (g) Qu, X. S.; Xu, L.; Gao, G. G.; Li, F. Y.; Yang, Y. Y. *Inorg. Chem.* **2007**, *46*, 4775–4777.
- (15) (a) Albrecht, M. *Chem. Rev.* **2001**, *101*, 3457–3498. (b) Torelli, S.; Delahaye, S.; Hauser, A.; Bernardinelli, G.; Piguat, C. *Chem.–Eur. J.* **2004**, *10*, 3503–3516. (c) Zeckert, K.; Hamacek, J.; Rivera, J. P.; Floquet, S.; Pinto, A.; Borkovec, M.; Piguat, C. *J. Am. Chem. Soc.* **2004**, *126*, 11589–11601. (d) Yeh, R. M.; Raymond, K. N. *Inorg. Chem.* **2006**, *45*, 1130–1139. (e) Fletcher, N. C.; Brown, R. T.; Doherty, A. P. *Inorg. Chem.* **2006**, *45*, 6132–6134. (f) Jensen, T. B.; Scopelliti, R.; Bunzli, J.-C. G. *Inorg. Chem.* **2006**, *45*, 7806–7814. (g) Zhang, J. P.; Zheng, S. L.; Huang, X. C.; Chen, X. M. *Angew. Chem. Int. Ed.* **2004**, *43*, 206–209.
- (16) Chen, B.; Eddaoudi, M.; Reineke, T. M.; Kampf, J. W.; O’Keeffe, M.; Yaghi, O. M. *J. Am. Chem. Soc.* **2000**, *122*, 11559–11560.

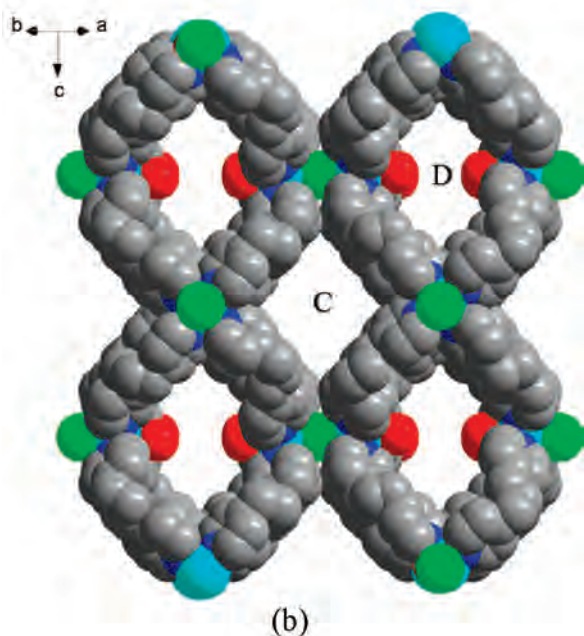
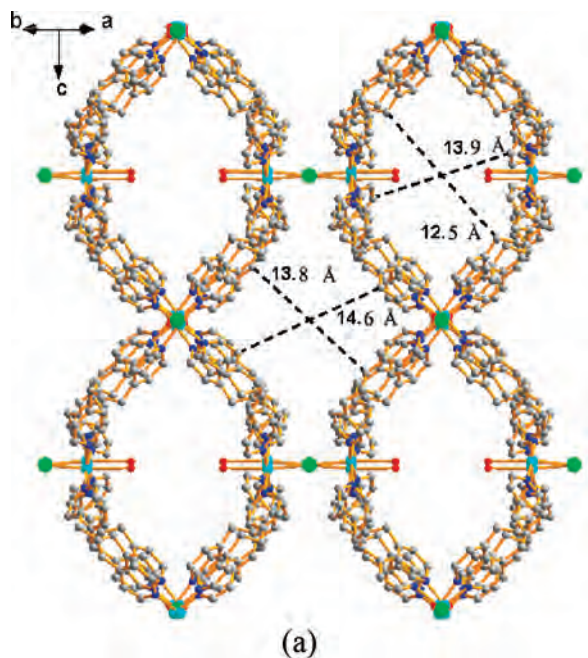


Figure 4. Ball-and-stick (a) and space-filling (b) representations of the channels in the 3-D cationic structure along the [110] direction. The channel sizes are dependent on the distance between C13, C14, C19, and C26 derived from bpp ligands and their symmetric operation atoms, respectively. The H atoms, the solvent-water molecules, and the Keggin-type ion templates are omitted for clarity.

elemental, ICP, and TG analyses (Figure 6, Supporting Information Figures S4 and S7–S10). As a result of the geometry of the bcc-type net of the cationic framework and the fcc-type structure of the stacking POMs,^{12,18} the combination of channels running parallel to each other gives rise to large pockets of extra-framework space. Analysis with the PLATON¹⁹ software tool indicates that the extra-framework volume per unit cell is approximately 36% (in the absence of water molecules). These large free spaces within the framework cause the structure to be highly porous;

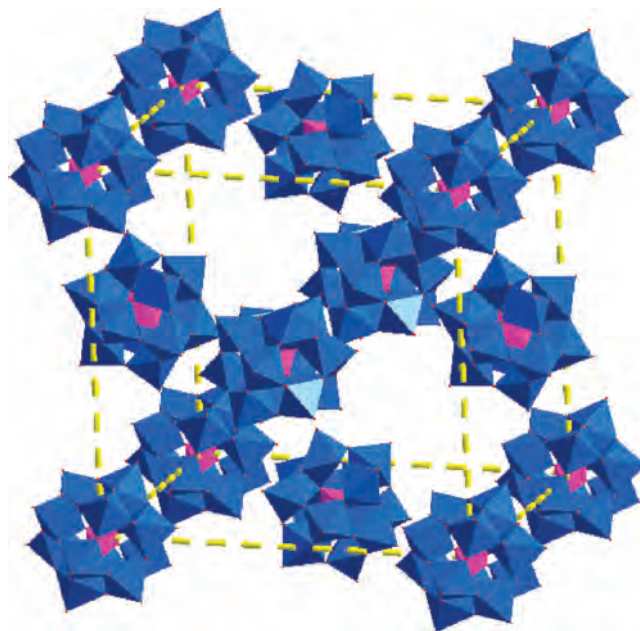


Figure 5. Polyhedral representation of a face-centered cube of the stacking POMs.

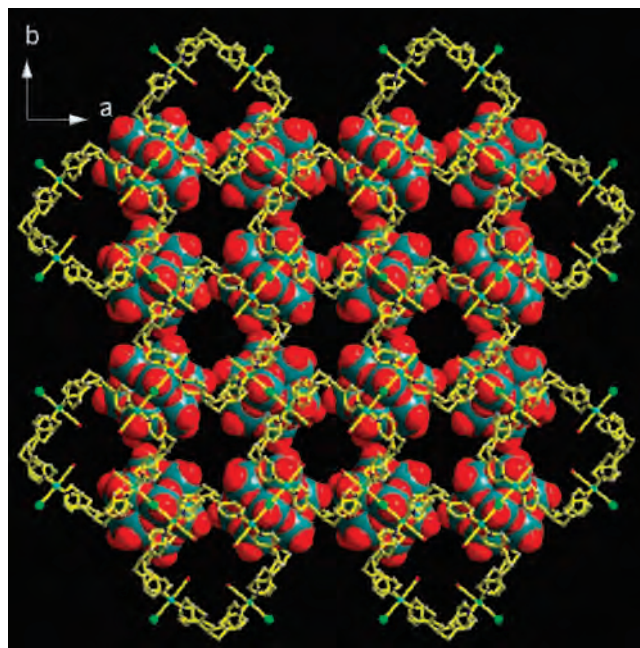


Figure 6. View of the [001] direction showing the 3-D network.

thus, the two compounds are perfect candidates for porous materials.

A better insight into the structures of the two title compounds can be obtained by the standard procedure of reducing multidimensional structures to simple node-and-

(17) (a) To better understand the overall net, we are simply to discuss the stacking mode of the POM anions, though there are no other obvious strong interactions between them. For a few representative examples, see L. FanXiao, D. R.; Li, Y. G.; Wang, E. B.; An, H. Y.; Su, Z. M.; Xu, L. *Inorg. Chem.* **2007**, *46*, 506–512. (b) Moulton, T. B.; Zaworotko, M. *J. Chem. Rev.* **2001**, *101*, 1629–1658; and references therein.

(18) Eddaoudi, M.; Kim, J.; O’Keeffe, M.; Yaghi, O. M. *J. Am. Chem. Soc.* **2002**, *124*, 376–377.

(19) Spek, A. L. *J. Appl. Crystallogr.* **2003**, *36*, 7.

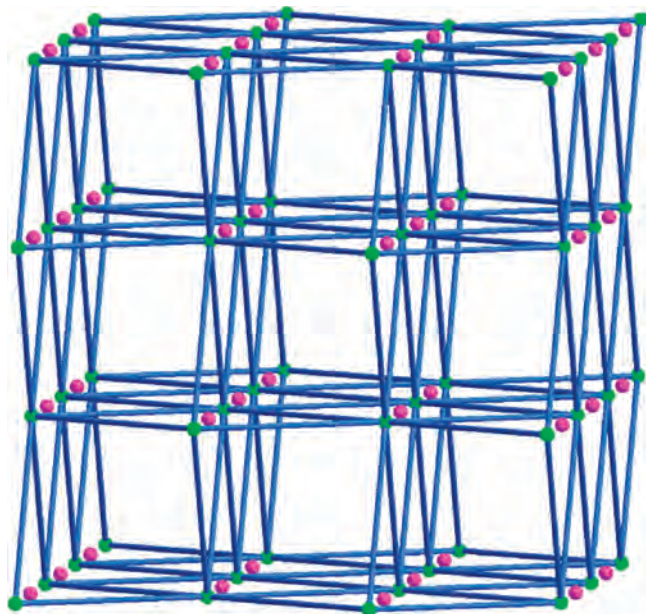


Figure 7. Representation of the eight-connected $4^{24} \cdot 6^4$ net of the 3-D polymer cations and the position of the POMs. Dinuclear unit, green; $[\text{PM}_{12}\text{O}_{40}]^{3-}$ cluster, purple.

linker reference nets known as the topological approach.^{14d,20} As shown above, each dinuclear unit is connected to adjacent units through eight bpp molecules along different directions. Therefore, each dinuclear unit can be defined as an eight-connected node. On the other hand, each $[\text{PM}_{12}\text{O}_{40}]^{3-}$ cluster is connected to twelve adjacent clusters via supramolecular interactions, and thus the Keggin-type anion can be regarded as a twelve-connected node (Supporting Information Figure S5). On the basis of this simplifications, the overall nets of **1** and **2** can be best rationalized as an eight-connected cationic framework with a body-centered cubic (Schläfli symbol $4^{24} \cdot 6^4$) stacking with a twelve-connected supramolecular structure with a face-centered cubic (Schläfli symbol $3^{24} \cdot 4^{36} \cdot 5^6$; Figure 7 and Supporting Information Figure S6).

In coordination chemistry, it is quite rare that high-connected cationic structures and 3-D organic–inorganic hybrid porous materials are assembled by directly incorporation of POMs as templates.²¹ The structures of **1** and **2** are unique with respect to the introduction of one of the largest noncoordinating anions and of the highest-connected coordination polymer cations to date in organic–inorganic hybrid materials, as well as in regard to the opportunities to use the removal/adsorption properties of the porous materials and the redox properties of the noncoordinating $[\text{PM}_{12}\text{O}_{40}]^{3-}$

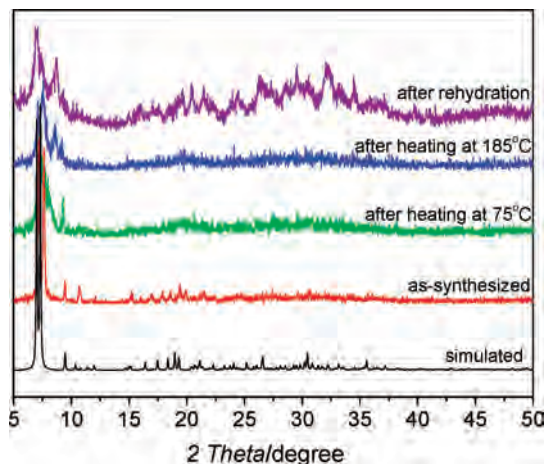


Figure 8. Powder XRD patterns of **1** after different treatment.

anions to carry out chemical reactions within the intercrystalline voids, avoiding disruption of the framework topology and crystallinity.

Powder X-ray Diffraction. Encouraged by the single-crystal X-ray diffraction results, which reveal large free spaces within the framework, we carried out powder X-ray diffraction experiment to investigate the stability of compound **1** upon the removal of guest molecules according to TG analysis. The XRD patterns indicate that the as-synthesized compound matches with the simulated one except for some intensity difference. The powder sample treated at 75 °C shows some indication of stability upon removal of part of the guest water molecules (ca. 1.3% weight loss); the differences, when compared to the as-synthesized one, may be reasoned as attributable to the removal of water molecules and the subtle change of the relative positions of some atoms in the crystal lattice.²² The sample heated at 185 °C (corresponding to 9.19% weight loss of all the water molecules) seems to lose crystallinity and collapse; this cannot be reversed after the treatment in water for 24 h because of the broadening and decrease of intensity of the peaks, thus producing an amorphous phase upon heating (Figure 8).

Photoluminescence Properties. Compounds **1** and **2** exhibit photoluminescent properties at ambient temperature (Supporting Information Figure S11). Two prominent emission peaks of both compounds are observed at about 405 and 460 nm upon excitation at 332 nm, showing similar emissions. In accordance with the photoluminescent properties of copper–bpp-related compounds and POMs,^{9b,23} the emission peak at about 460 nm can be assigned to photoluminescence signal of the free ligand bpp, and emissions at about 405 nm may be attributed to ligand-to-metal charge transfer.

(20) (a) Blake, A. J.; Champness, N. R.; Hubberstey, P.; Li, W. S.; Withersby, M. A.; Schröder, M. *Coord. Chem. Rev.* **1999**, *183*, 117–138. (b) Qin, C.; Wang, X. L.; Wang, E. B.; Su, Z. M. *Inorg. Chem.* **2005**, *44*, 7122–7129.

(21) It is worth mentioning that, among all the POM-templated materials, large pores or channels formed in the cationic networks were either very small or occupied by POMs, and therefore, none of them is actually porous material. Férey's group recently reported a new zeolite-like solid that can encapsulate five Keggin-type anions in one pore. However, this porous material is not involved in the POM-template method, and no single-crystal structural information about positions of Keggin-type ions in the solid is provided. Férey, G.; Mellot-Draznieks, C.; Serre, C.; Millange, F.; Dutour, J.; Surblé, S.; Margiolaki, I. *Science* **2005**, *309*, 2040.

(22) (a) Reineke, T. M.; Eddaoudi, M.; Fehr, M.; Kelley, D.; Yaghi, O. M. *J. Am. Chem. Soc.* **1999**, *121*, 1651–1657. (b) Du, M.; Chen, S. T.; Bu, X. H. *Cryst. Growth Des.* **2002**, *2*, 625–629.

(23) (a) Ghosh, A. K.; Ghoshal, D.; Lu, T. H.; Mostafa, G.; Chaudhuri, N. R. *Cryst. Growth Des.* **2004**, *4*, 851–857. (b) Zhang, J.; Chen, Y. B.; Chen, S. M.; Li, Z. J.; Cheng, J. K.; Yao, Y. G. *Inorg. Chem.* **2006**, *45*, 3161–3163. (c) Liu, Q. Y.; Xu, L. *CrystEngComm* **2005**, *7*, 87–89. (d) Yamase, T. *Chem. Rev.* **1998**, *98*, 307–326. (e) Yamase, T.; Sugeta, M. *J. Chem. Soc. Dalton Trans.* **1993**, 759, 765.

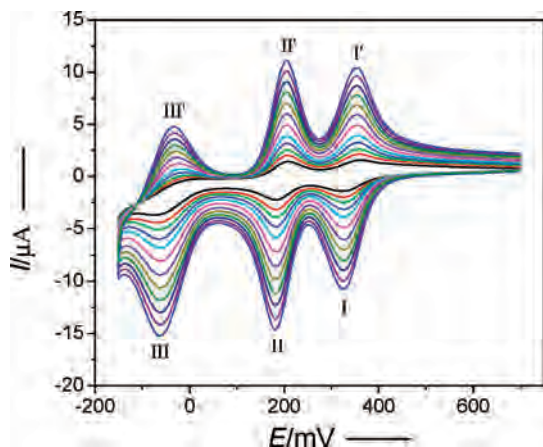


Figure 9. Cyclic voltammograms of the 2-CPE in the 1 M H₂SO₄ solution at different scan rates (from inner to outer: 50, 70, 90, 120, 150, 200, 250, 300, 350, 400, 450, 500 mV s⁻¹).

Electrochemical Properties. The electrochemical behavior of a 2-modified carbon paste electrode (2-CPE) and its electrocatalytic reduction of nitrite were investigated. The cyclic voltammetric behavior for 2-CPE in 1 M H₂SO₄ aqueous solution at different scan rates was recorded, exhibiting three reversible redox peaks in the potential range of +700 to -150 mV, attributable to the [PMO₁₂O₄₀]³⁻ polyanions (Figure 9).²⁴ The peak currents were proportional to the scan rate up to 500 mV s⁻¹, indicating that the redox process of 2-CPE is surface-controlled (Supporting Information Figure S12). As is well-known, the electroreduction of nitrite requires a large over potential,²⁵ and therefore no obvious response is observed in the range +700 to -150 mV on a bare CPE in 1 M H₂SO₄ aqueous solution containing 1 mM KNO₂ (Figure 10). However, 2-CPE displays good electrocatalytic activity toward the reduction of nitrite. On addition of NO₂⁻, all the reduction peak currents increase, and the corresponding oxidation peak currents decrease dramatically, which indicate that the three reduced species all show good electrocatalytic activity toward the reduction of nitrite.^{24,26} It is noteworthy that the third reduced species showed the best electrocatalytic activity, that is, the catalytic activity is enhanced with increasing extent of polyanion reduction (Figure 10 and Supporting Information Figure S13). It is also noted that 2-CPE possesses a high stability. The voltammetric behavior of the 2-CPE remains almost unchanged not only over 500 cycles at a scan rate of 100 mVs⁻¹ but also after it had been used for

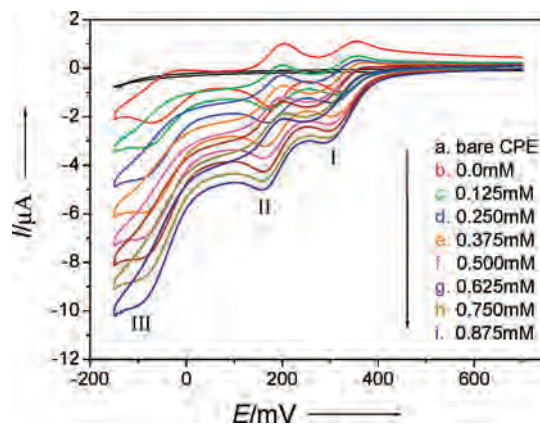


Figure 10. Cyclic voltammograms of the 2-CPE in 1 M H₂SO₄ solution containing 0.0–0.875 mM KNO₂ and a bare CPE in 1.0 mM KNO₂ and 1 M H₂SO₄ solution. Potentials vs SCE. Scan rate: 100 mVs⁻¹.

electrocatalytic reduction of nitrite and was then washed with a 1 M H₂SO₄ solution, suggesting that the host–guest structural feature of 2 stabilizes the Keggin-type ions in the compound.^{8c} Moreover, after 2-CPE was stored at room temperature for about 1 month, the peak current decreased only 6% and could be renewed by squeezing a little carbon paste out of the tube. This is especially useful for electrocatalytic studies, since the catalytic activity is known to decrease when the electrode is fouled.

In summary, compounds 1 and 2 represent the first examples of eight-connected organic–inorganic hybrid materials templated by Keggin-type anions. The novel linkage of the 3-D cationic network and POM-templates together with multifunctional properties of 1 and 2 make this species an interesting solid-state rarity. With hindsight, we can imagine that more of this kind of new hybrid materials could be prepared by replacement of Cu–bpp segments and/or by selection of different Keggin-type anions or other polyoxoanion templates. Further, if Keggin-type ion templates could be successfully removed or substituted by small anions without collapse of the host framework, much larger porous materials will be obtained. These efforts are currently ongoing.

Acknowledgment. This work was financially supported by National Postdoctoral Science Foundation of China (No. 2004035144), and the Natural Science Foundation of Liaoning Province of China (No. 20061073).

Supporting Information Available: X-ray crystallographic information files (CIF) for 1 and 2 and a PDF file. This material is available free of charge via the Internet at <http://pubs.acs.org>.

IC7014513

(24) (a) Wang, X. L.; Wang, E. B.; Lan, Y.; Hu, C. W. *J. Electroanal. Chem.* **2002**, 523, 142–149. (b) Wang, X. L.; Zhang, H.; Wang, E. B.; Han, Z. B.; Wang, L.; Hu, C. W. *Electroanalysis*. **2003**, 15, 1460–1464.

(25) Keita, B.; Nadjo, L. *J. Electroanal. Chem.* **1987**, 227, 77–98.

(26) Cheng, L.; Zhang, X. M.; Xi, X. D.; Dong, S. J. *J. Electroanal. Chem.* **1996**, 407, 97–103.